J|A|C|S
ARTICLES

# Nanoengineered Carbon Scaffolds for Hydrogen Storage

Ashley D. Leonard,[†] Jared L. Hudson,[†] Hua Fan,[†] Richard Booker,[†] Lin J. Simpson,[‡] Kevin J. O'Neill,[‡] Philip A. Parilla,[‡] Michael J. Heben,[‡] Matteo Pasquali,[†] Carter Kittrell,*[,†] and James M. Tour*[,†]

*Departments of Chemistry, Mechanical Engineering and Materials Science, Chemical and Biomolecular Engineering, and the Smalley Institute for Nanoscale Science and Technology, Rice University MS 222, 6100 Main Street, Houston, Texas 77005, and National Renewable Energy Laboratory, 1617 Cole Boulevard, Golden, Colorado 80401*

Received August 25, 2008; E-mail: kittrell@rice.edu; tour@rice.edu

***Abstract:*** Single-walled carbon nanotube (SWCNT) fibers were engineered to become a scaffold for the storage of hydrogen. Carbon nanotube fibers were swollen in oleum (fuming sulfuric acid), and organic spacer groups were covalently linked between the nanotubes using diazonium functionalization chemistry to provide 3-dimensional (3-D) frameworks for the adsorption of hydrogen molecules. These 3-D nanoengineered fibers physisorb twice as much hydrogen per unit surface area as do typical macroporous carbon materials. These fiber-based systems can have high density, and combined with the outstanding thermal conductivity of carbon nanotubes, this points a way toward solving the volumetric and heat-transfer constraints that limit some other hydrogen-storage supports.

## Introduction

Growing concerns regarding the accessibility of hydrocarbon fuels and their environmental impact have led to global interest in developing hydrogen-fueled vehicles.[1] Hydrogen can be an efficient energy carrier, and its sole reaction product in a fuel cell or internal combustion engine, being water, is pollution-free. Like gasoline, hydrogen is not a primary fuel; it must be generated from other sources. But unlike gasoline, hydrogen can be obtained from a wide variety of renewable energy protocols. Problematically, compressed hydrogen gas tanks are heavy and volumetrically large if they are to provide the equivalent energy content derivable from conventional liquid-filled gasoline tanks. Moreover, although currently being used in prototypes,[2,3] the use of high-pressure (5000 psi or 350 atm) hydrogen tanks in consumer automobiles lessens their attractiveness.

Hydrogen that is reversibly bound to a lightweight solid-phase support provides an attractive alternative to the large volume, weight, and pressure tanks currently being explored.[4] Although hydrogen could be generated onboard a vehicle by reforming hydrocarbons or by the catalytic decomposition of a chemical hydride, only fueling with hydrogen and the storage of this hydrogen will be considered here. This divides the storage of hydrogen into two basic categories: covalent binding (chemisorption) of the dissociated hydrogen, usually as a metal hydride, and physical adsorption (physisorption) of the hydrogen molecule. In the former case, covalent binding of the hydrogen atom to the metal is generally strong, which requires elevated temperatures to release the hydrogen. Nanoparticles are used for hydrogen chemisorption because of their high surface areas coupled with the ability to have good kinetics for the adsorption and release of hydrogen.[5,6] However, the metal nanoparticles tend to be unstable with hydrogen depletion and are prone to aggregation, causing poor cycling. Conversely, the undissociated hydrogen molecule can be physisorbed onto a high-surface-area porous structure of lightweight materials, and carbon is the most widely explored system. This is both in the amorphous carbon form (usually activated) and $sp^2$-carbon-rich systems that include both graphite and carbon nanotubes.[7] Metal−organic frameworks (MOFs) can also provide high surface areas for physisorption of hydrogen.[8] In general, these materials utilize reduced temperatures to adsorb the hydrogen molecule, as the binding of molecular hydrogen to the surface is relatively weak. The intermediate case is termed spillover in which the hydrogen molecule is catalytically dissociated and the atomic hydrogen migrates onto a host surface. It is then catalytically recombined for delivery as a hydrogen molecule. The dissociation on platinum or similar catalyst takes place at room temperature, and the uptake and release of hydrogen is accomplished through a change in pressure.[9,10] Although this has the desirable property of storing and releasing hydrogen at room temperature, the kinetics of uptake tend to be slow, which would lead to extended fill times, and the quantity stored has been less than that achieved by physisorption at reduced temperatures.

[†] Rice University.
[‡] National Renewable Energy Laboratory.

(1) Hefner, R. A., III. *Int. J. Hydrogen Energy* **2002**, *27*, 1–9.
(2) http://world.honda.com/FuelCell/FCX/tank/ (accessed August 7, 2008).
(3) Kamiya, I.; Mori, R.; Kudo, M. Compressed Hydrogen Tank for Fuel Cell Vehicle. JP67457, Aug 31, 2007.
(4) Morris, R. E.; Wheatley, P. S. *Angew. Chem., Int. Ed.* **2008**, *47*, 4966–4981.
(5) Berube, V.; Radtke, G.; Dresselhaus, M.; Chen, G. *Int. J. Energy Res.* **2007**, *31*, 637–663.
(6) Seayad, A. M.; Antonelli, D. M. *Adv. Mater.* **2004**, *16*, 765–777.
(7) Stroebel, R.; Garche, J.; Moseley, P. T.; Joerissen, L.; Wolf, G. *J. Power Sources* **2006**, *159*, 781–801.
(8) Wong-Foy, A. G.; Matzger, A. J.; Yaghi, O. M. *J. Am. Chem. Soc.* **2006**, *128*, 3494–3495.
(9) Li, Y.; Yang, R. T. *J. Am. Chem. Soc.* **2006**, *128*, 8136–8137.
(10) Li, Y.; Yang, R. T. *Langmuir* **2007**, *23*, 12937–12944.

  

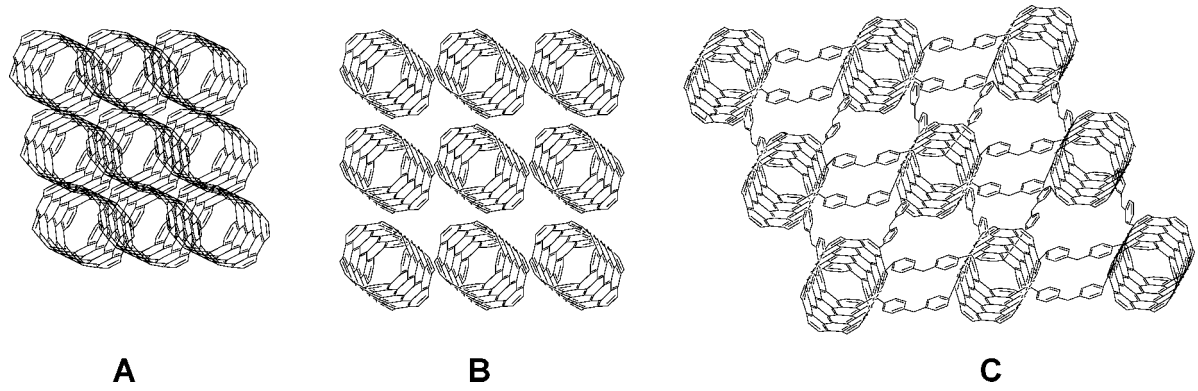


***Figure 1.*** Illustration showing the cross-sectional view of a SWCNT fiber. (A) The individual tubes in the fiber are packed tightly in the bundle, maximizing the density of the fiber. (B) A fiber where the SWCNTs have debundled slightly because of oleum intercalation, thereby expanding the fiber diameter. (C) The SWCNT fiber is locked into this slightly debundled form through functionalization with cross-linkers.

The use of physisorption rather than chemisorption of hydrogen atoms to a surface eliminates the need for high heating to desorb the hydrogen from the solid phase, thereby providing faster kinetics of release. This also provides high energy efficiency and essentially complete availability of all stored hydrogen at lower pressures, generally in the 1−100 atm range. In addition, it is desirable to have a storage medium that is stable upon cycling, that can provide good thermal conductivity to dissipate the heat of adsorption, and that has paths with minimal tortuosity for fast kinetics of uptake. Although many solid-phase supports have been prepared, they are neither high density nor do they have high thermal conductivity for heat removal during the adsorption step.[4] We show here the fabrication of chemically cross-linked 3-dimensional (3-D) frameworks of single-walled carbon nanotube (SWCNT) fibers. These fibers physisorb twice as much hydrogen, at low pressures, with respect to their surface areas, than typical macroporous carbon materials.

SWCNT fibers alone do not have sufficient surface area for the storage of hydrogen because the SWCNTs are bundled tightly together (Figure 1A). The fibers can swell in oleum (20% free $SO_3$, fuming sulfuric acid) (Figure 1B), which protonates the nanotube surfaces and intercalates between them, overcoming the van der Waals attractions of 0.5 eV/nm cohesive interaction between adjacent nanotubes,[11−13] and causing the fiber diameter to expand. If recoagulated in water, the fibers repack and return approximately to their starting diameter (Figure 1A). The swollen geometry could be locked-in by inserting cross-links that are stable in oleum,[11] yielding fibers with an expanded geometry and stabilized enlarged pores even after removal of the intercalating solvent (Figure 1C). It is the interstitial spaces between nanotubes (Figure 1C) that could be tuned by the choice of intercalating acid and cross-linker, providing higher surface area for hydrogen adsorption and also a multifaced environment for the hydrogen to assume several points of physisorption contact.

The production of SWCNT fibers is known from previous work.[14] SWCNTs can be dispersed in oleum to form liquid-crystalline dopes and spun into well-aligned fibers using conventional spinning techniques much like those for making aramid fibers such as Kevlar.[14,15] Because of alignment, SWCNTs in fibers have a considerably better packing density than in powders. The SWCNT fibers have densities of about 1.0−1.2 g/cm$^3$, and they have packing densities of 70−80%, thereby well-addressing the volumetric desires for mobile adsorption beds.[14,16] The alignment of the SWCNTs in the fibers creates a path of low tortuousity for hydrogen diffusion, leading to faster kinetics of uptake. Powders tend to be poor thermal conductors due to the lack of connectivity between the particles, whereas continuous fibers are better suited to benefit from the high uniaxial thermal conductivity of the individual carbon nanotubes. For these reasons, SWCNT-based structures of this type have recently been theorized by Weck et al. to be thermodynamically stable and good choices for the storage of hydrogen.[17]

## Results and Discussion

The chemistry taking place on the SWCNTs is shown in eq 1, where methylenedianiline is converted, in situ, into the bis-diazonium salt which can add between adjacent nanotubes in the bundled structure of the fiber (Figure 1C). This particular cross-linker was chosen because its end-to-end distance would provide a 7−9 Å spacing which is in the range desired for molecular hydrogen packing[17] and because its rigidity would limit its intratube attachment. Ring sulfonation on the anilines during oleum functionalizations occurs as described previously.[11,18−20]

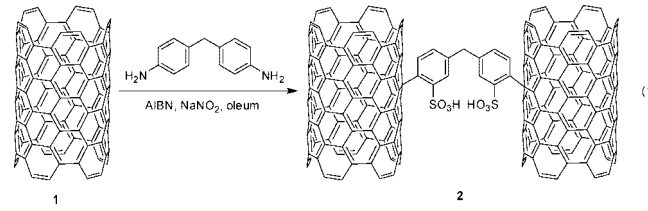


This creates expansion between the individual SWCNTs, thus providing greater surface area for hydrogen adsorption. The functionalization of the SWCNT fibers is confirmed using Raman spectroscopy.[12,19] The D-band (diamondoid) at 1290 cm$^{-1}$ is diagnostic for the sp$^3$-hybridized carbons, compared to the G-band (graphitic) at 1594 cm$^{-1}$ that is diagnostic for the sp$^2$-hybridized carbons remaining on the SWCNTs. An increase in the D/G ratio in Raman spectra of these fibers is indicative of functionalization of SWCNTs. After functionalization of the SWCNT fibers, the D/G increases from 0.05 to 0.17 as shown in Figure 2, confirming covalent functionalization.

(11) Hudson, J. L.; Casavant, M. J.; Tour, J. M. *J. Am. Chem. Soc.* **2004**, *126*, 11158–11159.
(12) Bahr, J. L.; Tour, J. M. *J. Mater. Chem.* **2002**, *12*, 1952–1958.
(13) Liu, T.; Kumar, S. *Nano Lett.* **2003**, *3*, 647–650.

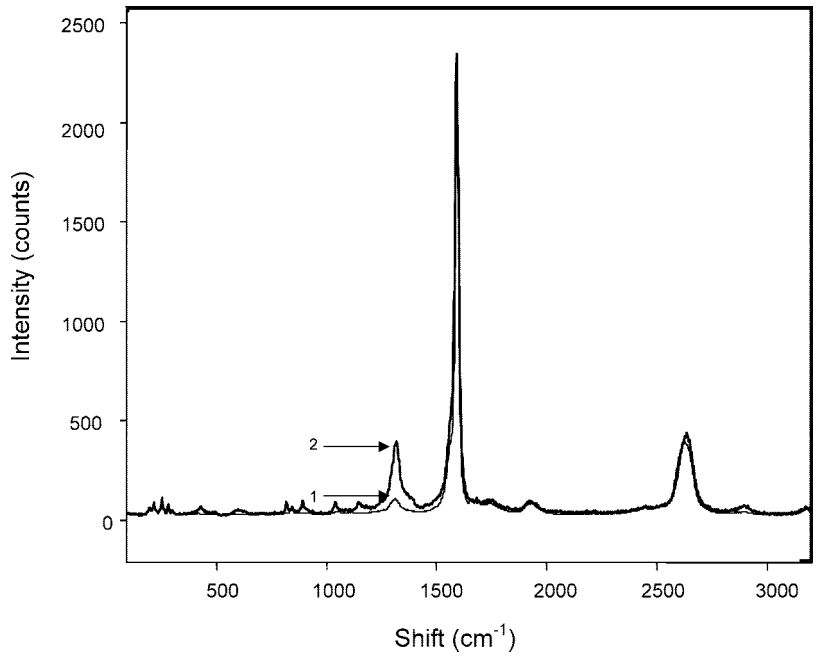


***Figure 2.*** Representative Raman spectrum (633 nm excitation) showing the starting SWCNT fiber **1** and cross-linked product **2**. The increase in the D band in **2** is indicative of sidewall functionalization of the nanotubes that comprise the fiber.

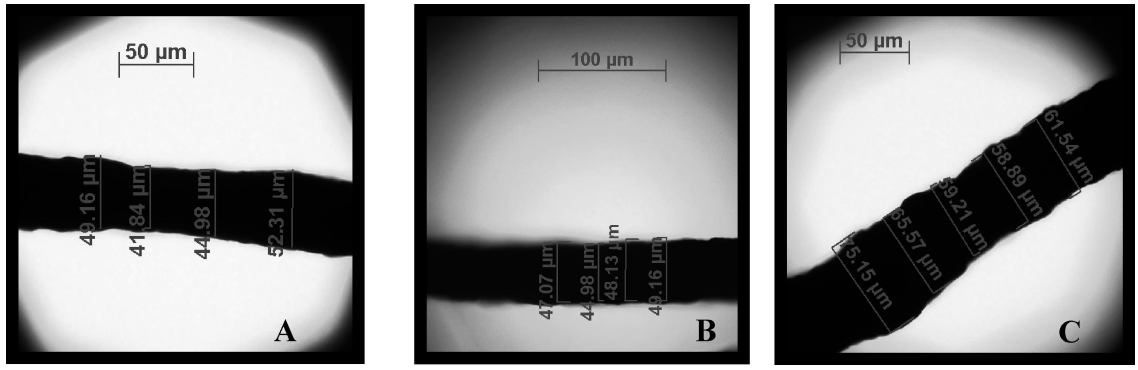


***Figure 3.*** Optical micrographs of a SWCNT fiber before and after functionalization with methylenedianiline to build the 3-D nanoengineered structure. (A) SWCNT fiber before functionalization; average diameter = 47 $\mu$m. (B) The same SWCNT fiber after expansion in oleum and subsequent recoagulation in water without having been exposed to the cross-linking spacer group; average diameter = 47 $\mu$m. (C) SWCNT fiber after expansion in oleum, functionalization using methylenedianiline in the same solvent, and then coagulation into water to remove oleum; average diameter = 65 $\mu$m. A 30−40% increase in the fiber diameter was maintained through the covalent cross-linking of several samples.

Typically, SWCNT fibers have diameters of 40−200 $\mu$m;[14] therefore, optical microscopy can be used to measure the expansion of the fibers after functionalization. As shown in Figure 3, the starting SWCNT fiber average diameter is 47 $\mu$m (Figure 3A). When this fiber is expanded in oleum and then is plunged back into water, it coalesces back to its near-original average diameter of 47 $\mu$m (Figure 3B). After oleum intercalation and functionalization, this SWCNT fiber retains an average diameter of 65 $\mu$m (Figure 3C), an increase of ~30%. These functionalized fibers remain expanded, and they do not fall apart even at temperatures as high as 800 °C under hydrogen and argon. Though 300−500 °C is typically sufficient to remove all aryl pendants from a SWCNT via evolution of an aryl radical,[20] in this case, the chelation effect and the restricted environments deter loss of the addend from the inner cavities. Desulfonation is expected to occur upon heating to these temperatures. However, the cross-linking prevents collapse of the scaffold so there is no energy assist from recovery of the van der Waals interaction, thus making it even more difficult to drive out the sulfuric acid solvent.

The methylenedianiline-functionalized SWCNT fiber (**2**) was tested for hydrogen-adsorption capacity at 2 bar and 77 K; surprisingly there was only 0.03 wt % hydrogen uptake. At this stage, the expanded SWCNT fibers were "sticky", consistent with trapped sulfuric acid in the pores of the SWCNT fibers. Using thermogravimetric analysis (TGA) to heat the functionalized SWCNT fibers to 600 °C under argon, a weight loss of 45 wt % was seen (Figure 4), which is attributed to the evaporation of intercalated sulfuric acid with some desulfonation and loss of the peripheral addends.

The liberation of trapped sulfuric acid and/or sulfonic acid moieties was confirmed by the observation of sulfur-containing species during thermal desorption mass spectroscopy. Thereafter, the functionalized SWCNT fibers were heated either under vacuum or an inert atmosphere to remove the trapped acid from the scaffolds and allow for the adsorption of hydrogen. The expanded structure of the fibers was kept intact after heating as determined by optical diameter measurements. Thus, we can conclude that the internal cross-linkers are not destroyed during the heating process.

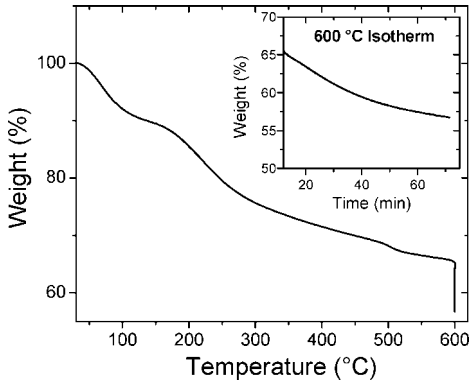


***Figure 4.*** Thermogravimetric analysis of the functionalized SWCNT fibers heated under argon at a heating rate of 10 °C/min to 600 °C and held there for 1 h. A weight loss of 45 wt % is attributed to the evaporation of intercalated sulfuric acid and desulfonation of the cross-linker.

***Table 1.*** Heating of Functionalized SWCNT Fibers Produces Higher BET Surface Areas after Removal of the Sulfuric Acid[a]

| heating temperature (°C) | surface area ($m^2$/g) |
|---|---|
| 200 | 218 |
| 350 | 347 |
| 500 | 396 |
| 650 | 501 |
| 800 | 515 |

[a] The conditions involve heating the same sample in a BET analyzer under vacuum and holding for 12 h, or for temperatures above 350 °C, the sample was heated in a furnace for 30 min under argon and 10% hydrogen before recording the BET surface area.

In order to determine if the trapped sulfuric acid was causing the poor hydrogen adsorption, the functionalized fibers were heated to increasingly higher temperatures, and the BET surface area was recorded as shown in Table 1. When the fibers were heated to a minimal temperature of 200 °C, the nitrogen BET surface area was found to be 218 $m^2$/g whereas when the temperature was significantly increased to 800 °C, the surface area increased to 515 $m^2$/g, an increase of 130%. The boiling point of sulfuric acid is 338 °C, and is given as a rough guide. Even when the fibers are baked under vacuum, which will lower the temperature for outgassing, it is more than offset by the strong physisorption into the sticky $sp^2$-carbon pores of the expanded lattice. Since the rigid framework cannot collapse, there is no recovery of the large tube−tube van der Waals interaction, and hence there is no energy of collapse that could otherwise drive out the acid upon heating.

Hypothesizing that the cross-linkers could be preventing the escape of trapped acid and blocking hydrogen from penetrating into the fibers, we also used a complementary functionalization scheme: decreasing the amount of cross-linker and replacing it with a small, noncross-linking moiety produced from 4-chloroaniline in order to keep the SWCNT fibers propped open. After a few experiments, the preferred ratio of cross-linker (methylenedianiline) to chloroaniline was found to be 1:9, which kept the SWCNT fibers propped open to the same degree by optical microscopy measurements but presumably created more space for the trapped acid sulfur species to depart the fiber. Through this study we found that it is important to retain some cross-linked SWCNT fibers to maintain sample integrity. When the SWCNT fibers were functionalized with only 4-chloroaniline, the fibers retained no structural integrity and they could no longer be handled without falling apart. This confirms that simply adding functional groups to the walls of the SWCNTs does not lead to a stable expanded structure; cross-linking units are essential. Decreasing the amount of cross-linker and replacing it with 4-chloroaniline presumably allowed for the trapped sulfuric acid to be removed from the fibers, an assumption which was confirmed with a higher hydrogen uptake.

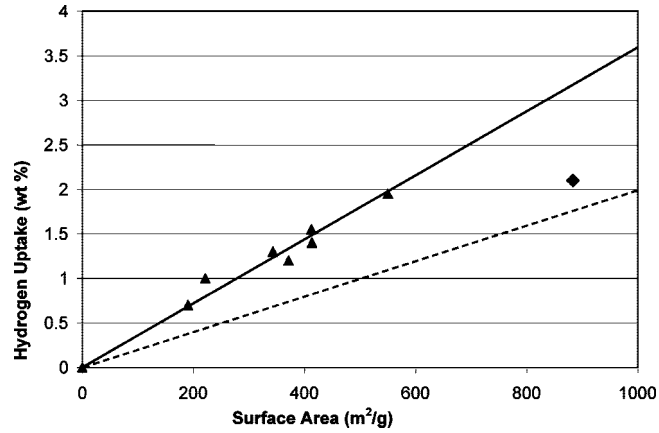


***Figure 5.*** Specific surface area determined from nitrogen BET at 77 K versus hydrogen uptake at 77 K and 2 bar. The solid line is the fit and extrapolation obtained from our samples (triangles). The dashed line correlates to the maximum surface excess values typically observed for macroporous carbons. The diamond is the data point obtained with the fluorinated fibers.

As shown in Figure 5, a variety of nanoengineered SWCNT fiber samples were prepared using the oleum functionalization chemistry with methylenedianiline and chloroaniline (1:9) and hydrogen uptake measurements were performed after the sulfuric acid was thermally removed. Although the physical size differences between hydrogen and the larger nitrogen are realized, standardization to common BET methods was sought. Hydrogen vs nitrogen size difference is a problem that we share in common with the other researchers making and testing nanoporous materials to store hydrogen. However, it behooves us to use the same nitrogen-based BET method which is the most widely used measurement technique for surface area. Moreover, since we have obtained the hydrogen uptake numbers and they correlate well with the BET-derived data, the comparisons between the two gases appear reasonable in this case.

Plotting the surface area of the samples against the average hydrogen uptake at 2 bar and 77 K provides a fitted line slope that is significantly steeper than that typically found for surface adsorption onto other macroporous carbon materials. As determined by Chahine et al., typical activated carbon materials show a maximum surface excess of ∼1 wt % hydrogen for every 500 $m^2$/g of specific surface area at 30−50 bar.[21] Thus, for a

(14) (a) Ericson, L. M.; Fan, H.; Peng, H.; Davis, V. A.; Zhou, W.; Sulpizio, J.; Wang, Y.; Booker, R.; Vavro, J.; Guthy, C.; Parra-Vasquez, A. N. G.; Kim, M. J.; Ramesh, S.; Saini, R. K.; Kittrell, C.; Lavin, G.; Schmidt, H.; Adams, W. W.; Billups, W. E.; Pasquali, M.; Hwang, W.-F.; Hauge, R. H.; Fischer, J. E.; Smalley, R. E. *Science* **2004**, *305*, 1447–1450. (b) Davis, V. A.; Ericson, L. M.; Parra-Vasquez, A. N. G.; Fan, H.; Wang, Y.; Prieto, V.; Longoria, J. A.; Ramesh, S.; Saini, R. K.; Kittrell, C.; Billups, W. E.; Adams, W. W.; Hauge, R. H.; Smalley, R. E.; Pasquali, M. *Macromolecules* **2004**, *37*, 154–160.
(15) Murata, K.; Kaneko, K.; Kanoh, H.; Kasuya, D.; Takahashi, K.; Kokai, F.; Yudasaka, M.; Iijima, S. *J. Phys. Chem. B* **2002**, *106*, 11132–11138.
(16) Wang, Y.; Ericson, L. M.; Kittrell, C.; Kim, M. J.; Shan, H.; Fan, H.; Ripley, S.; Ramesh, S.; Hauge, R. H.; Adams, W. W.; Pasquali, M.; Smalley, R. E. *Chem. Mater.* **2005**, *17*, 6361–6368.
(17) Weck, P. F.; Kim, E.; Balakrishnan, N.; Cheng, H.; Yakobson, B. I. *Chem. Phys. Lett.* **2007**, *439*, 354–359.

typically activated carbon with ~2500 $m^2/g$, a maximum surface excess of ~5 wt % hydrogen is expected according to this so-called "Chahine rule".

Due to the limited sample quantities produced in these laboratory-scale experiments (5−20 mg), we needed to use a more accurate volumetric measurement system that has an upper pressure limit of ~2 bar (see Experimental Section). Hence, the uptake values reported here are expected to be significantly below the maximum surface excess values. Yet, on a per specific surface area basis, the sorbed amount is nearly a factor of 2 greater than the amount expected from consideration of the Chahine slope (dashed line, Figure 5). For comparison purposes, purified laser-generated SWCNTs which were extensively processed with acid and base washes and high temperature treatments in air or $CO_2$ resulted in high surface areas of ~800 $m^2/g$ and sorbed ~2 wt % hydrogen at 2 bar and 77 K and have a maximum surface excess hydrogen uptake of ~3 wt %. This suggests that the uptake values reported in Figure 5 could be scaled by an additional 23–33% to project the saturation surface excess values at higher pressures.[22] Such an adjustment would make the slope we obtained in Figure 5 substantially steeper than the 1.85 wt % uptake per 500 $m^2/g$ that we obtained at 2 bar.

These data demonstrate that when hydrogen is taken up into nanometer-sized pores that are surrounded by $sp^2$ carbon, as in the case for these scaffolded SWCNTs, there is a considerable enhancement of hydrogen adsorption. If extrapolated, there would be 3.7 wt % hydrogen uptake with 1000 $m^2/g$ and 7.4 wt % hydrogen uptake at 2000 $m^2/g$ using only 2 bar of pressure. Thus, it appears that the key to designing a carbon-based hydrogen-adsorption medium is not only relying on the surface area of the material but also on engineering the pore size to be optimal for hydrogen adsorption.

In order to assess the role of the $\pi$-electron cloud of the SWCNT fibers in storing hydrogen on the scaffold, we heavily functionalized the fibers with fluorine[23] (26 at. % fluorine by X-ray photoelectron spectroscopy, XPS) causing the $\pi$-electron cloud to be significantly destroyed. The resulting fibers have a high specific surface area of 883 $m^2/g$ but the hydrogen adsorption of 2.1 wt % (diamond in Figure 5) falls below the line derived from the data in the present work but close to the Chahine slope. Therefore, preserving the $sp^2$-carbon structure of the individual SWCNT in the fibers appears important for the higher storage of hydrogen.

Our samples are not at all identical. Each expanded scaffold was deliberately prepared from a different batch of spun SWCNT fiber; the amount of expansion also varied, the functionalization was changed, and the total hydrogen wt % uptake exhibits a wide range. Yet, in spite of these many variations, the data points are all remarkably consistent in their proximity to the enhanced slope illustrated in Figure 5. The one thing that is consistent throughout all of these measurements is that the hydrogen is enveloped in a $\pi$-cloud of $sp^2$ carbon. However, when the $\pi$-cloud was disrupted as shown by the addition of fluorine to the scaffold that converts a large portion of the $sp^2$ carbons to $sp^3$ carbons, the enhancement was lost along with the $\pi$-cloud for this control experiment. Similar enhanced uptake of hydrogen was reported by the Iijima group[15] for isolated pockets of hydrogen surrounded by $sp^2$ carbons in adjacent nanohorns and in calculations by the Seifert and Heine.[24,25] Likewise, the Eklund group[26] observed over a factor of 2 enhancement in binding energy for those hydrogen molecules fully intercalated into a carbon nanotube bundle compared to those bound to just a single surface of a SWCNT on the outside of the bundle. Therefore, our observed need for high degrees of $sp^2$-carbon atoms in the nanopores corroborates well with the body of literature data on the subject.

Although the work presented here shows the 3-D scaffolds to be superior in comparison to unordered SWCNTs, the challenge of removing trapped sulfuric acid still leads us to investigate alternative functionalization methods where we might achieve higher surface areas and concomitant hydrogen adsorption weights. Finally, with these carbon scaffolds in hand, we are using them as platforms for supporting metals in order to enhance the uptake of hydrogen at ambient temperatures.

## Summary

Scaffolds for the storage of hydrogen have been engineered by swelling SWCNT fibers and cross-linking the open structures in place, thereby providing a 3-D nanoengineered network. These scaffolds double the amount of hydrogen that can be adsorbed, per unit surface area, over typical macroporous carbon frameworks. The SWCNT scaffolds have the high density needed to pack hydrogen into a small amount of space. Work is underway to synthesize the SWCNT fibers with better pore sizes for the storage of hydrogen, with the ultimate goal of developing a hydrogen vehicle fuel tank that works near ambient temperature and pressure.

## Experimental Section

**General.** Purified SWCNTs[27] were obtained from Rice University HiPco laboratory. Oleum was purchased from Alfa Aesar. All other starting compounds were purchased from Sigma-Aldrich and used without further purification. TGA was performed using a heating rate of 10 °C/min under argon. Raman spectroscopy was performed on a Renishaw in Via Raman microscope using a 633 nm He−Ne laser, taking the median of five scans. Optical microscope images were taken using a polarizing optical microscope (Zeiss Axioplan-2). Multipoint BET measurements recorded in Table 1 were taken using 11 points on a Quantachrome Autosorb-3b BET surface analyzer using nitrogen at 77 K. The BET surface areas recorded on this instrument were within 10% of the BET surface areas obtained in the Quantachrome Autosorb-1 Physisorption system noted below. XPS analysis was carried out on a PHI Quantera SXM Scanning X-ray Microprobe with a pass energy of 26.00 eV, 45° takeoff angle, and 100 $\mu$m beam size. Samples were evacuated prior to XPS analysis at room temperature and 0.1 mm Hg for 12 h, and these conditions were also used before testing for uptake. The SWCNT fibers were spun according to the previously described protocol.[14] **CAUTION**: *Oleum is a dangerous and corrosive liquid. The user should wear a laboratory coat, a rubber smock, thick-lined rubber gloves, eye protection, and a full-face shield. All reactions should be conducted using a well-ventilated*

(18) Stephenson, J. J.; Hudson, J. L.; Leonard, A. D.; Price, B. K.; Tour, J. M. *Chem. Mater.* **2007**, *19*, 3491–3498.
(19) Dyke, C. A.; Tour, J. M. *J. Phys. Chem. A* **2004**, *108*, 11151–11159.
(20) (a) Dyke, C. A.; Tour, J. M. *Carbon Nanotubes* **2006**, 275–294. (b) Dyke, C. A.; Tour, J. M. Functionalized Carbon Nanotubes in Composites. In *Carbon Nanotubes: Properties and Applications*; O'Connell, M. J., Ed., CRC: New York, 2006; pp 275−294.
(21) Benard, P.; Chahine, R. *Int. J. Hydrogen Energy* **2001**, *26*, 849–855.
(22) (a) Parilla, P. A.; Dillon, A. C.; Gennett, T.; Alleman, J. L.; Jones, K. M.; Heben, M. J. *Mater. Res. Soc. Symp. Proc.* **2001**, *633*, A14 36 11A14 36 16. (b) Simpson, L. J.; Parilla, P. A.; Blackburn, J. L.; Gennett, T. G.; Gilbert, K. E. H.; Engtrakul, C.; Dillon, A. C.; Heben, M. J. *Global Progress Toward Clean Energy: Proceedings of the 17th NHA Annual Hydrogen Conference, 12−16 March 2006, Long Beach, California (DVD-ROM)*; National Hydrogen Association: Washington, DC, 2006; p 14.
(23) Mickelson, E. T.; Huffman, C. B.; Rinzler, A. G.; Smalley, R. E.; Hauge, R. H.; Margrave, J. L. *Chem. Phys. Lett.* **1998**, *296*, 188–194.

*hood with the sash down and the reaction mixture behind a secondary transparent shield. Likewise, fluorine gas is very reactive and corrosive and it should be used only with approved gas fittings and manifold as previously described.*[28]

**Hydrogen Uptake Measurements.** All hydrogen uptake measurements were recorded at the National Renewable Energy Laboratory using a home-built system[22] that records hydrogen uptake at 2 bar and 77 K while simultaneously providing the ability to heat-treat and record BET surface areas on the same sample without exposure to air. The critical advance in this instrument which allows high-precision measurements on very small (<5 mg) samples is the direct control of the temperature and temperature gradients across the various zones using copper collars, graphoil gaskets, and a closed-loop thermostatted heat exchanger. The BET specific surface areas where measured using a Quantachrome Autosorb-1 Physisorption system that had all of the O-rings sealed, electrically actuated valves replaced with metal-sealed and pneumatically actuated valved systems to improve thermal stability and accuracy to achieve BET measurements on small samples. Temperature-programmed desorption was performed using a custom-built system.

**Methylenedianiline-Functionalized SWCNT Fibers (2).** SWCNT fibers (49 mg, 4.1 mequiv C) and 20 mL of oleum (20% free $SO_3$) were placed in a 150 mL crystallization dish on an orbital shaker under nitrogen for 30 min. In a separate vial, methylenedianiline (0.813 g, 4.1 mmol) was dissolved in oleum (2 mL) and was then carefully added to the fiber suspension. Following the addition of the aniline, sodium nitrite (0.57 g, 8.2 mmol) and 2,2′-azobis(2-methylpropionitrile) (AIBN, 0.135 g, 0.82 mmol) were carefully and sequentially added, and the fibers were mixed under nitrogen on the orbital shaker for 1 h. After 1 h, the reaction mixture was quenched by carefully pouring it over ice. The fibers were then filtered over a polycarbonate membrane (0.22 $\mu$m pores), and the fibers were rinsed several times with water (30 mL), followed by methanol (30 mL) and ether (30 mL). Once rinsed, the fibers were dried under vacuum (0.1 mmHg) for 12 h. The Raman D/G ratio was 0.17.

**1:9 Methylenedianiline and Chloroaniline-Functionalized SWCNT Fibers (3).** SWCNT fibers (24 mg, 2.0 mequiv C) and 20 mL of oleum (20% free $SO_3$) were placed in a 150 mL crystallization dish under nitrogen, allowing the oleum to intercalate in the SWCNT fibers for 30 min on an orbital shaker. In a separate vial, methylenedianiline (0.020 g, 0.1 mmol) and 4-chloroaniline (0.115 g, 0.9 mmol) were dissolved in 2 mL of oleum and the mixture was then carefully added to the fibers. Following the addition of the anilines, sodium nitrite (0.166 g, 2.4 mmol) and AIBN (0.039 g, 0.12 mmol) were carefully and sequentially added and the mixture was shaken under nitrogen for 1 h. The same workup as above afforded the desired fibers. The Raman D/G ratio was 0.47.

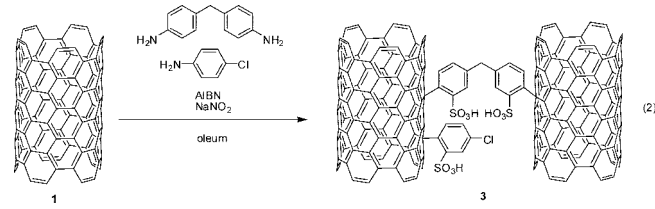


**Fluorinated SWNT Fibers (4).** A similar procedure for fluorination of SWNCTs was followed.[23] Briefly, SWCNT fibers (18 mg) were placed in a Monel reactor. The apparatus was flushed with helium while the system was slowly heated to 70 °C at which point fluorine was introduced to the system. Fluorine flowed through the system for 1.5 h. After this time, the flow of fluorine was stopped and the reactor was slowly cooled under helium gas flow to room temperature. Once at room temperature, the sample was removed and no purification was needed. The Raman D/G ratio was 0.34. XPS: C = 53.9%, F = 25.9%, O = 20.1%.

**Acknowledgment.** Financial support provided by the U.S. Department of Energy's Office of Energy Efficiency and Renewable Energy within the Hydrogen Sorption Center of Excellence, DE-FC-36-05GO15073, and from the Air Force Office of Scientific Research, FA9550-06-1-0207.

JA806633P

(24) Patchkovskii, S.; Tse, J. S.; Yurchenko, S. N.; Zhechkov, L.; Heine, T.; Seifert, G. *Proc. Nat. Acad. Sci. U.S.A.* **2005**, *102*, 10439–10444.
(25) Kuc, A.; Zhechkov, L.; Patchkovskii, S.; Seifert, G.; Heine, T. *Nano Lett.* **2007**, *7*, 1–5.
(26) Pradhan, B. K.; Sumanasekera, G. U.; Adu, K. W.; Romero, H. E.; Williams, K. A.; Eklund, P. C. *Physica B* **2002**, *323*, 115–121.
(27) Chiang, I. W.; Brinson, B. E.; Huang, A. Y.; Willis, P. A.; Bronikowski, M. J.; Margrave, J. L.; Smalley, R. E.; Hauge, R. H. *J. Phys. Chem. B* **2001**, *105*, 8297–8301.
(28) Lagow, R. J.; Badachhape, R. B.; Wood, J. L.; Margrave, J. L. *J. Am. Chem. Soc.* **1974**, 1268–1273.